Molecularly Imprinted Sensor based on Ag-Au NPs/SPCE for Lactate Determination in Sweat for Healthcare and Sport Monitoring

Liping Zhou

Sports Institute, Henan University of Technology, Zhengzhou, 450000, China
E-mail: zhouliping201407@163.com

This study presented fabrication of wearable amperometric lactate sensor based on molecularly imprinted polymer on Ag-Au nanoparticles (MIP/Ag-Au NPs) modified screen-printed carbon electrodes (SPCE) for sweat analysis in healthcare and sport monitoring. For modification of SPCE, the chemical synthesized Ag and Au NPs were spin-coated on SPCE, and MIPs electropolymerized on Ag-Au NPs/SPCE surface. Structural and morphological analyses by SEM, XRD and EDS confirmed that spherical Ag-Au nanoparticles were distributed homogeneously on the of MIP molecules. Electrochemical studies by CV and amperometry techniques indicated that the synergetic effect of the modification of the Ag-Au NPs with MIP particles were resulted in larger electroactive sites on the surface and improve the stability, selectivity and analytical signal because of their direct and fast electron transfer between a substrate and electrochemical ions. The linear range, detection limit and sensitivity of lactate sensor was obtained of 1-220µM, 0.003µM and 0.88066µA/µM, respectively. The performance of the proposed flexible sensor was examined after applied mechanical forces and results demonstrated great durability and stability under the twisting and bending. MIP/Ag-Au NPs/SPCE sensor was attached to volunteers' skin for the monitoring of the lactate level during cycle exercise and obtained results suggested that MIP/Ag-Au NPs/SPCE as feasible and reliable wearable sensor can be used for continuously monitoring of lactate level in sweat.

1. INTRODUCTION

Recent developments in microelectronics, nanotechnology and data processing have provided new opportunities for application of flexible wearable platforms in a medical device for healthcare through continuous monitoring of physiological parameters [1-3]. Recent researches have been conducted on promote and miniaturization of physiological monitoring systems to assess the pulse,

electrocardiography, skin temperature, blood pressure, oxygen saturation, bodily motion and respiratory rate from the human epidermis [4-6].

Wearable chemical and electrochemical sensors are devices that convert chemical and electrochemical information into analytical signals [7-9]. Moreover, studies have been indicated that wearable epidermal electrochemical sensors can help to analyze the lactate, potassium, glucose, ammonia, alcohol, cortisol and urea levels in human sweat for healthcare and sport monitoring [10, 11]. Between these chemical components, lactate ($C_3H_6O_3$) as an important component of intermediary metabolism is related to sports performance and training regimens which is the byproduct of the metabolism of glucose by muscle cells [12, 13].

During high physical activity and higher exercise intensity, the glucose flux increase into the cell because of high contractile demands by skeletal muscle to produce energy which leads to the production of a higher level of lactate [14-16]. Furthermore, lactate is a biomarker of tissue perfusion and oxygenation because it is a byproduct of anaerobic glycolysis in inadequate oxygen delivery and tissue hypoxia [17-19]. Studies have been shown that the lactate concentrations are from 10 to 70 mM for sporting applications [20, 21]. Monitoring lactate can help to prevent pulmonary embolism and hemorrhagic shock in endurance and high strength activities. Therefore, this study was focused on the fabrication of wearable amperometric sensors MIP/Ag-Au NPs/SPCE as lactate sensors for sweat analysis in healthcare and sport monitoring.

2. MATERIALS AND METHOD

2.1. Synthesis of MIPs/Ag-Au NPs on screen-printed carbon electrode

All chemicals were purchased from Sigma-Aldrich (St. Louis MO, USA). In order to preparation Ag NPs [22, 23], 0.4g pyrrole monomer and 4.5g $AgNO_3$ (99.0%), 0.5g $FeCl_3$ (99%) was dissolved into 50mL of ethylene glycol (≥99%). This mixture was stirred at 120ºC for 2 hours. After the reaction, the resulted product was cooled at room temperature, and then 2 mL glycerol (≥99.5%), 10mL N-methyl pyrrolidone (99.5 %), 5 mL poly(vinylpyrrolidone) (≥99%) and 25mL ethylene glycol were added to the resulted product under magnetic stirring and the stirring was continued at room temperature for 5 hours. After then, the obtained Ag NPs was centrifuged at 1500 rpm for 5 minutes. Next, Ag NPs were rinsed with deionized water and ultrasonically dispersed in ethanol (99.8%) to achieve the 10 mg/mL of dispersed Ag NPs mixture, respectively. Subsequently, the dispersed Ag NPs were stored at dark and room temperature for further use.

For the synthesis of Au NPs using the microwave heating method [24], 1 ml $HAuCl_4$ (≥99.9%) solution and 1 ml $Na_3C_6H_5O_7$ (≥99%) solution was ultrasonically added to 20ml deionized water. Then, the solution was transferred into the microwave oven chamber (KMFD264TEX, Electrolux Co., Stockholm, Sweden) at 190 W for 15 minutes. The obtained powder was ultrasonically dispersed in ethanol to obtain the 10 mg/mL of dispersed Au NPs suspension.

The screen-printed carbon electrode (SPCE, Dalian Thrive Mining Co., Ltd., China) was used as a substrate which was fabricated on flexible polyethylene terephthalate (PET) substrate. To

modification the SPCE with MIPs/Ag-Au NPs, the mixture of 0.1mL of the dispersed Ag NPs and 0.1mL of the dispersed Au NPs in the equal ratio was dropped onto the SPCE and were spin-coated at a rotating speed of 400 rpm for 1minute. Next, the electrode was dried at 70ºC for 60 minutes. Subsequently, the electropolymerization was applied for deposition of MIPs was on the Ag-Au NPs spin-coated SPCE using the cyclic voltammetry (CV) technique on CHI660E electrochemical workstation (CH Instruments Inc., China) in three-electrode cell under applied potential range from −0.5 V to +0.5 V at a scan rate of 30 mV/s in for 50 cycles in the prepared polymeric electrolyte. Three-electrode cell was contained carbon as working electrode, Pt wire as counter electrode and Ag/AgCl as a reference electrode. The electropolymerization electrolyte was prepared from 0.04 g 3-aminophenyl boronic acid (99%), 0.1g lactic acid as template and 0.2 g NaCl (*99%*) which were ultrasonically dissolved in 15 mL of 0.1 M PBS solution pH 7.3. For pre-polymerization, the prepared solution was kept in the darkness for 5 hours. After electropolymerization, the MIP/Ag-Au NPs/SPCE was immersed in acetonitrile (99%) at room temperature for 2 minutes to remove the embedded template molecules and create recognition imprinted cavities which allow better access to the analyte molecules [25].

2.2. Characterization

CV and amperometry experiments were conducted on CHI660E electrochemical workstation using a three-electrode system which contained prepared electrodes as working electrode, Pt wire as counter electrode and Ag/AgCl as a reference electrode. 0.1M PBS was used as an electrolyte for electrochemical studies which prepared from an equal volume ratio of 0.1 M NaH_2PO_4 (99%) and 0.1 M Na_2HPO_4 (99.95%). Scanning electron microscopy (SEM; Hitachi S-4700II, Tokyo, Japan) and X-ray diffraction (XRD; Bruker-AXS, Billerica, MA, USA) analyses were used to characterization the structural and surface morphologies of the prepared electrodes. Energy dispersive x-ray spectroscopy (EDS) analysis was performed for study the elemental and chemical study of the samples using a Bruker X Flash 6 solid-state EDX.

3. RESULT AND DISCUSSION

Figure 1 shows the SEM images of Ag-Au NPs/SPCE and MIP/Ag-Au NPs/SPCE. Figure 1a exhibits the SEM images of the Ag-Au NPs spin-coated SPCE which indicated uniformly formation of Ag-Au nanoparticles with a size of 100-200nm on the porous surface of SPCE. As observed from Figure 1b, the metal nanoparticles are distributed homogeneously on the MIP molecules with a high surface coverage. MIP surface with a higher surface area, more cavities and pore volume leads to a higher adsorption capacity [26, 27]. Elimination of the template molecules in MIP network with strategically positioned functional groups in binding sites causes to more interacting with the very small analyte molecules in a strong and the selective way [28, 29].
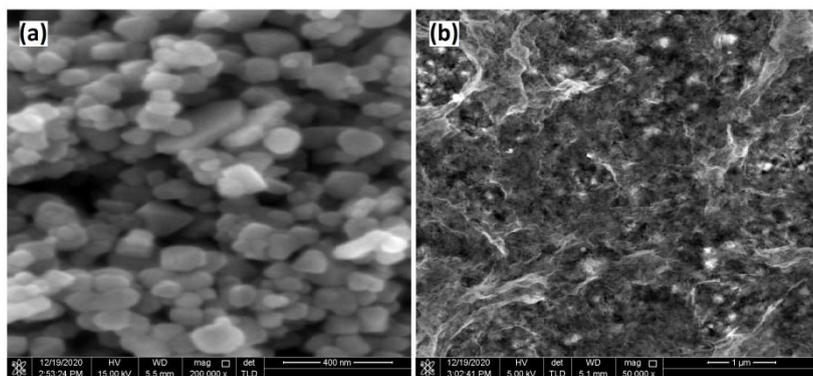
Figure 1. SEM images of (a) Ag-Au NPs/SPCE and (b) MIP/Ag-Au NPs/SPCE.

Figure 2 presents the XRD patterns of SPCE, Au NPs/SPCE, Ag NPs/SPCE, Ag-Au NPs/SPCE and MIP/Ag-Au NPs/SPCE. As seen, the XRD patterns of all samples show diffraction peak at 26.19° which is associated with (002) plane of graphitic structure of SPCE(JCPDS card No. 12-0212). XRD pattern of Au NPs/SPCE in Figure 2b displays diffraction peaks at 38.29°, and 41.97° that these are related to (111) and (200) planes of face-centered cubic (fcc) phase of Au nanoparticles, respectively (JCPDS card No. 03-0921) [30]. XRD pattern ofAg NPs/SPCEinFigure2c shows diffraction peaks at 38.1°, 44.3° and 64.5°which attributed to (111), (200),(220) and (311) planes of fcc phase of Ag nanoparticles (JCPDS card No. 04-0783). The XRD patterns of Au–Ag NPs/SPCE, and MIP/Ag-Au NPs/SPCE are shown in Figures 2d and 2e display the same patterns with the diffraction peaks at 38.02°, 44.11°, 64.89° and 77.29° indicating to (111), (200) and (220) crystallographic planes of Au–Ag alloy NPs crystalline in nature [31, 32]. The XRD patterns of MIP/Ag-Au NPs/SPCE shows lower peak densities due to amorphous phases of the polymer system in MIP [33].
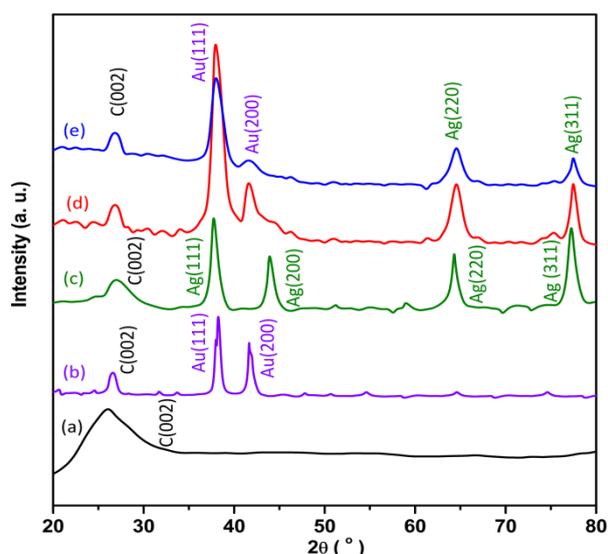

Figure 2. XRD patterns of (a) SPCE, (b) Au NPs/SPCE, (c) Ag NPs/SPCE, (d) Ag-Au NPs/SPCE and(e) MIP/Ag-Au NPs/SPCE.

EDS spectra of MIP/Ag-Au NPs are presented in Figure 3. As observed, there are the Ag and Au elements in the EDS spectrum. Moreover, the signals of C and O elements are observed that related to MIP layer [34]. The results of SEM, XRD and EDS analyses confirm to successful formation the bimetallic Ag-Au NPs and hybrid structure MIP/Ag-Au NPs/SPCE.
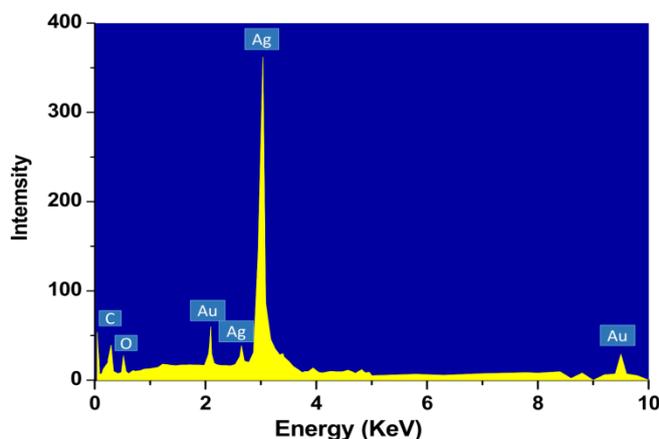
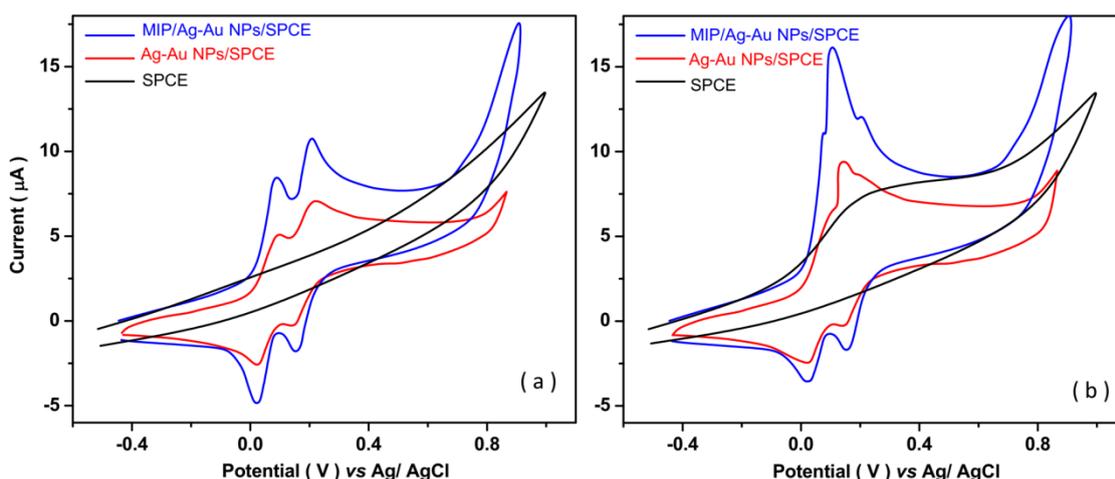

Figure 3. EDS spectra of MIP/Ag-Au NPs/SPCE.

Figure 4. CV curves of SPCE, Ag-Au NPs/SPCE and MIP/Ag-Au NPs/SPCE in 0.1M PBS pH 7.4 at 20 mV/s scan rate (a) before and (b) after addition of 5μM lactate solution.

Figure 4 displays the CV curves of SPCE, Ag-Au NPs/SPCE and MIP/Ag-Au NPs/SPCE in 0.1M PBS pH 7.4 at 20 mV/s scan rate before and after addition of lactate solution. Before the addition of lactate solution (Figure 4a), the CV curve of SPCE show no significant peak. The CV of Ag-Au NPs/SPCE and MIP/Ag-Au NPs/SPCE show two cathodic peaks at 0.08V and 0.20V that attributed to oxidation of Ag^0 into Ag^+ and Au^0 into Au^+ [35], respectively, and two anodic peaks at 0.02 V and 0.15 V that attributed to the reduction of Ag^+ to Ag^0 and reduction of Au^+ to Au^+ [35], respectively. As seen, there is the higher surrounded area by CV curves of the MIP/Ag-Au NPs/SPCE that it related to

the higher effective surface area of the electrode due to the formation of the microporous framework and more accessible imprinted cavities [36, 37]. Moreover, the synergetic effect of the modification of the Ag-Au NPs with MIP particles has resulted in a larger electroactive sites on surface and improve the analytical signal because of their direct and fast electron transfer between a substrate and electrochemical ions that is in agreement with the results of SEM analyses [38, 39].

After addition of 5µM lactate solution (Figure 4b), the CV curves exhibit the oxidation peak of lactate at 0.23, 0.14 and 0.1 V for SPCE, Ag-Au NPs/SPCE and MIP/Ag-Au NPs/SPCE, respectively that attributed to electrochemically oxidation of lactate is oxidized to pyruvate [40, 41]. Comparison between the CV responses of SPCE and Ag-Au NPs/SPCE presents the Ag-Au NPs role on the increase of two times peak current to the determination of lactate that it may be related to higher conductivity and effective surface area of metallic nanoparticles on SPCE [42, 43].The comparison between the CV curves of Ag-Au NPs/SPCE and MIP/Ag-Au NPs/SPCE reveals that the imprinted polymer matrix enhances the electrocatalytic currents due to generation cavities with certain ligands on the polymer that can act as specific receptors (binding sites) which can be directly attached to the analyte [44]. The combination of spin-coated Ag-Au NPs and MIP remarkably promotes the conductivity, and create the specific molecular recognition sites of cavities positioned in polymer network on Ag-Au NPs surface improves delectability [42, 44].
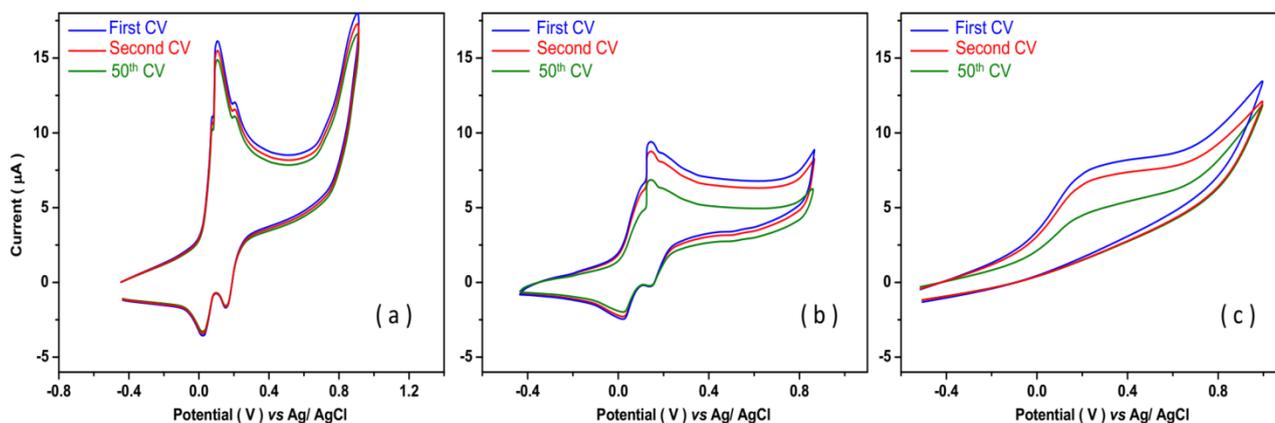

Figure 5. First, second and 50th CV curves of SPCE, Ag-Au NPs/SPCE and MIP/Ag-Au NPs/SPCE in 0.1M PBS pH 7.4 containing 5µM lactate solution at 20 mV/s scan rate.

The stability of response of SPCE, Ag-Au NPs/SPCE and MIP/Ag-Au NPs/SPCE to addition 5 µM lactate solution was examined through the record of continues CV scans in 0.1 M PBS pH 7.4 at 20 mV/s scan rate. Figure 5 displays the first, second and 50th scans of electrodes which indicated the change of peak current between the first and second scans is negligible. However, the decrease in oxidation current peaks after continues 50 scans is36%, 27% and 7% for SPCE, Ag-Au NPs/SPCE and MIP/Ag-Au NPs/SPCE, respectively, indicating the great stability of MIP/Ag-Au NPs/SPCE because of MIP's inherent advantages such as high mechanical stability and direct bonding of the MIP during electropolymerization of polymer on metallic nanoparticles using monomers with double bonds or

molecules [45]. Therefore, the further electrochemical studies were conducted on MIP/Ag-Au NPs/SPCE as lactate sensors.

Figure 6 shows the amperometric response and obtained calibration graph of MIP/Ag-Au NPs/SPCE to successive addition of 10μM lactate solution in 0.1 M PBS pH 7.4 at 0.1 V.As seen; the amperometric response is linearly increased with increasing the lactate concentration from 1 to 220 μM. In addition, the detection limit and sensitivity are obtained of 0.003μM and 0.88066 μA/ μM, respectively. The obtained sensing results in this study are compared with the other reported lactate sensors in literature in Table 1. As observed, the highest sensitivity is belonging to the MIP/Ag-Au NPs/SPCE that is related to the synergetic effect of the Ag and Au NPs with MIP which create high conductivity and large electroactive sites on the SPCE surface.
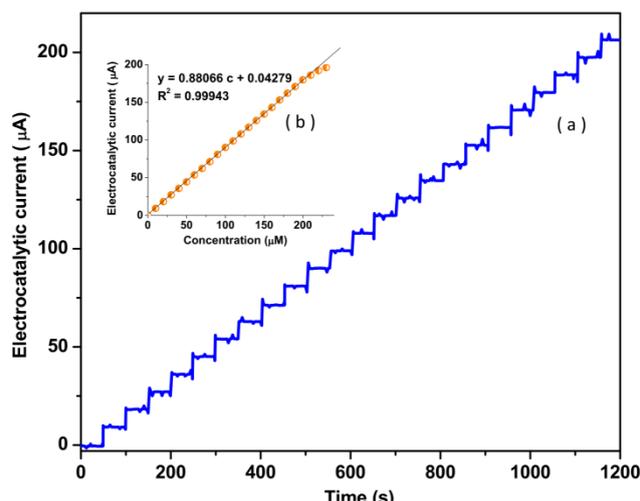

Figure 6. (a) Amperometric response and (b) obtained calibration graph of MIP/Ag-Au NPs/SPCE to successive addition of 10μM lactate solution in 0.1 M PBS pH 7.4 at 0.1 V.

Table 1. Comparison between the obtained sensing results in this study and the other reported lactate sensors in literatures

Electrode	Technique	Linear Range (μM)	limit of detection (μM)	Sensitivity (μA/μM)	Ref.
MIP/Ag-Au NPs/SPCE	Amperometry	1 – 220	0.003	0.88066	This work
nickel-metal organic framework	Amperometry	1000–4000	5	0.02953	[46]
MIP/Au NPs/rGO/GCE	DPV	0.0001–0.001	0.09	0.19	[47]
nicotinamide adenine dinucleotide/lactate dehydrogenase /Nano-CeO$_2$/GCE	Amperometry	200–2000	50	0.57119	[48]
hollow sphere structured	Amperometry	0.5 – 88.5	0.023	0.1179	[49]

NiS					
Lactate oxidase/dithiobis-N-succinimidyl propionate/macroporous Au film	Amperometry	100– 1300	3.93	0.00149	[50]
Lactate dehydrogenase/Meldola blue/MWCNT	Amperometry	1000– 10000	7.5	0.000415	[51]
Lactate oxidase/mesoporous silica/Co phthalocyanine/SPCE	Amperometry	74.0 −1500	18.3	-	[52]

The repeatability and selectivity of MIP/Ag-Au NPs/SPCE as lactate sensor was investigated using amperometry technique in 0.1 M PBS pH 7.4 at 0.1 V in successive addition of lactate and several metabolic substances in the human sweat as interfering agents such as urea (10mM), glucose (0.17mM), pyruvic acid (0.18mM), uric acid (0.05 mM),KCl (6 mM), NaCl (30mM), CaCl$_2$ (5mM), MgCl$_2$(0.08mM) and NH$_4$Cl(5 mM) in their physiological concentration [53]. The lactate level in human sweat has been reported from 16 mM on the face to over 30 mM in normal people on the thigh during strenuous exercise [54]. It is observed from Figure 7 that the amperometric response is considerably increased after the first addition of 1 μM lactate solution (∼0.88 μA) and recorded amperometric responses of the sensor to the interference substances are negligible, indicating the interfering agents do not interfere with the detection of lactate on MIP/Ag-Au NPs/SPCE. Finally, the amperometric response is increased for the second addition of 1 μM lactate solution as last addition (∼0.91 μA) that it implied to good repeatability and high stability of MIP/Ag-Au NPs/SPCE to the determination of lactate. In the electropolymerization process, the polymeric chains and template molecules are trapped within the 3D polymer matrix.
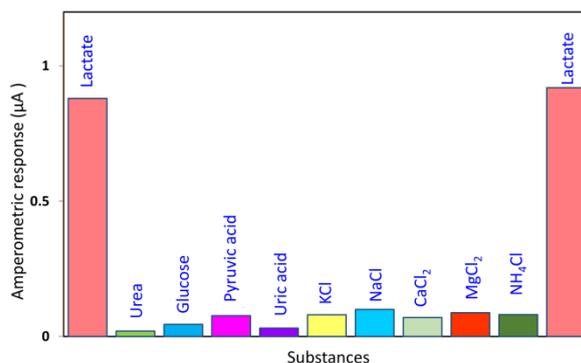

Figure 7. The amperometry response of MIP/Ag-Au NPs/SPCE in 0.1 M PBS pH 7.4 at 0.1 V in successive addition of lactate and several metabolic substances in the human sweat as interfering agents

After removing the template, ideally leaving selective recognizing sites that is complementary to the target species. In the presence of lactate molecules, the polymer matrix of MIP is cross-linked with the surface sites that can bind selectively to certain ligands on the polymer [38, 44, 45]. Moreover, the amperometric response of the second addition of lactate solution is slightly more than its first addition that it could be related to the increase of the ionic concentration in the solution after the addition of salt interferents [55].

The performance of the proposed flexible lactate sensor was examined after applied 180° twisting and bending as mechanical forces. Figure 8 shows the relative amperometric response (I_2/I_1) of MIP/Ag-Au NPs/SPCE in 0.1 M PBS pH 7.4 at 0.1 Vafter15 times of twisting or bending, where I_1 and I_2 are the amperometric currents of the electrode before and after applied mechanical forces, respectively. It is observed that the relative responses show recovery of 0.986 and 0.978 after subjected twisting and bending 150 times, respectively. Thus, MIP/Ag-Au NPs/SPCE demonstrates great durability and stability under the twisting and bending that it is an important parameter for continuous monitoring of lactate levels during exercise on the body's skin.
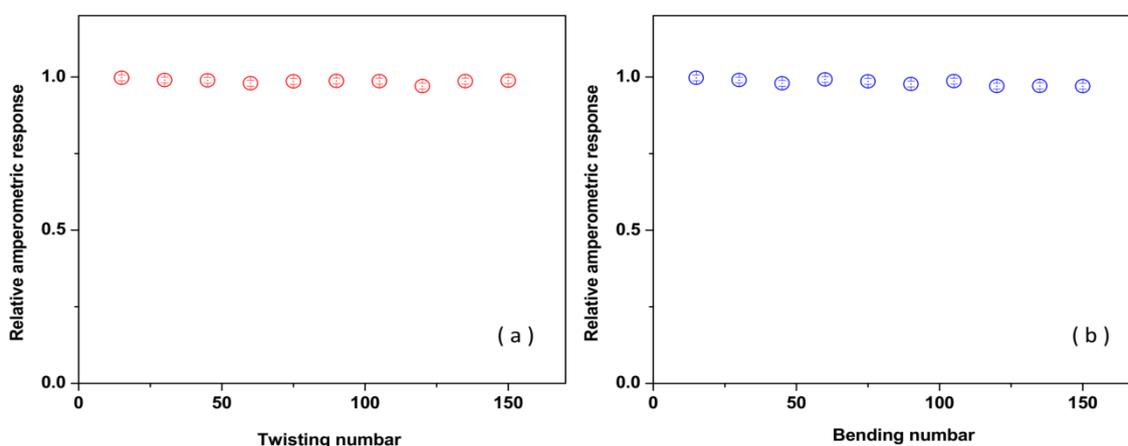

Figure 8. Relative amperometric responses of MIP/Ag-Au NPs/SPCE in 0.1 M PBS pH 7.4 at 0.1 V after repeated inward (a) twisting and (b) bending 150 times.

For fabrication of the wearable three-electrode electrochemical *lactate* sensor, MIP/Ag-Au NPs/SPCE as working, Ag/AgCl ink as reference and Pt as counter electrodes were printed on the thin film. A thin line of MIP/Ag-Au NPs/SPCE as working, a thin line of carbon as counter and a thin line of Ag/AgCl inks as reference were manually deposited onto the PET. The prepared wearable lactate sensor with a sweat cell was attached to the arm of volunteer aged twenty years through stretchable polydimethylsiloxane (200 μm) thin film. Heart rates were continuously recorded and monitored during cycle exercise (Figure 9a). The change of sweat lactate content was monitored by amperometry technique every 10 minutes during the cycling exercise. Figure 9b shows that there is no amperometric signal during the first 10 minutes of exercise because of insufficient sweat. After 10 minutes of cycle exercise, the amperometric signal is increased because of sufficient sweat and the

lactate production from the sweat. There is a gradual decrease of amperometric signal after 30 minutes which is related to the decrease of heart rate and exercise intensity. After 30 minutes exercise, the concentration of lactate in sweat can be estimated as 17.2 mM by considering the calibration plots in Figure 6b. These measurements were repeated for 4 young volunteers aged 18 to 20 years and results displayed the similar amperometric responses (Table 2). The obtained results suggested that MIP/Ag-Au NPs/SPCE as feasible and reliable wearable sensors can be used for continuously monitoring lactate levels in sweat. In addition, it wasn't observed any irritation or inflammation of the skin during the electrochemical measurements.
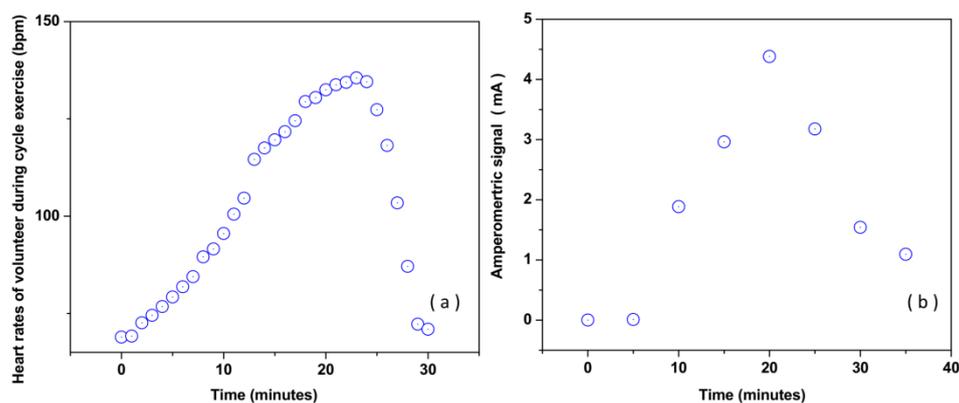

Figure 9. (a) Heart rates of volunteer during cycle exercise; (b) the amperometric signal of MIP/Ag-Au NPs/SPCE to change of sweat lactate content in 0.1 M PBS pH 7.4 at 0.1 V

Table 2. Analytical results of amperomertry studies of MIP/Ag-Au NPs/SPCE to determination lactate content in prepared real samples of sweat of 5 young volunteers aged 18 to 20 years in 0.1 M PBS pH 7.4 at 0.1 V after 30 minutes.

Sample	concentration of lactate in sweat (mM)	RSD (%)
S1	17.2	1.02
S2	16.9	0.96
S3	17.2	0.88
S4	17.1	0.98
S5	17.3	1.05

4. CONCLUSION

This study was focused on the fabrication of wearable amperometric sensors MIP/Ag-Au NPs/SPCE as lactate sensors for sweat analysis in healthcare and sport monitoring. For modification of SPCE, the chemical synthesized Ag and Au NPs were spin-coated on SPCE, and MIPs electropolymerized on Ag-Au NPs/SPCE surface. Results of structural and morphological analyses showed that spherical Ag-Au nanoparticles were distributed homogeneously on the MIP molecules. Results of electrochemical studies illustrated that the synergetic effect of the modification of the Ag-

Int. J. Electrochem. Sci., 16 **(2021)** Article Number: 211043

11

Au NPs with MIP particles resulted in larger electroactive sites on the surface and improve the stability, selectivity and analytical signal because of their direct and fast electron transfer between a substrate and electrochemical ions. The linear range, detection limit and sensitivity of lactate sensor were obtained of 1-220 µM, 0.003 µM and 0.88066µA/µM, respectively. The performance of the proposed flexible sensor was examined after applied mechanical forces and results demonstrated great durability and stability under the twisting and bending. MIP/Ag-Au NPs/SPCE sensor was attached on volunteers' skin for the monitoring of the lactate level during cycle exercise and obtained results suggested that MIP/Ag-Au NPs/SPCE as feasible and reliable wearable sensor can be used for continuously monitoring of lactate level in sweat.

References

1. L. Wang, K. Jiang and G. Shen, *Advanced Materials Technologies*, 24 (2021) 2100107.
2. C. Zhang, L. Li and J. Ou, *Structural Control and Health Monitoring*, 17 (2010) 549.
3. Y. Orooji, B. Tanhaei, A. Ayati, S.H. Tabrizi, M. Alizadeh, F.F. Bamoharram, F. Karimi, S. Salmanpour, J. Rouhi and S. Afshar, *Chemosphere*, 281 (2021) 130795.
4. S. Majumder, T. Mondal and M.J. Deen, *Sensors*, 17 (2017) 130.
5. Q. Wang, S. Sun, X. Zhang, H. Liu, B. Sun and S. Guo, *Bioresource Technology*, 332 (2021) 125120.
6. H. Karimi-Maleh, Y. Orooji, F. Karimi, M. Alizadeh, M. Baghayeri, J. Rouhi, S. Tajik, H. Beitollahi, S. Agarwal and V.K. Gupta, *Biosensors and Bioelectronics*, 184 (2021) 113252.
7. F. Zhao, T. Sun, F. Geng, P. Chen and Y. Gao, *International Journal of Electrochemical Science*, 14 (2019) 5287.
8. C. Gong, Y. Hu, J. Gao, Y. Wang and L. Yan, *IEEE Transactions on Industrial Electronics*, 67 (2019) 5913.
9. H. Karimi-Maleh, M.L. Yola, N. Atar, Y. Orooji, F. Karimi, P.S. Kumar, J. Rouhi and M. Baghayeri, *Journal of colloid and interface science*, 592 (2021) 174.
10. D.R. Seshadri, R.T. Li, J.E. Voos, J.R. Rowbottom, C.M. Alfes, C.A. Zorman and C.K. Drummond, *NPJ digital medicine*, 2 (2019) 1.
11. L. Zhang, M. Zhang, S. You, D. Ma, J. Zhao and Z. Chen, *Science of The Total Environment*, 780 (2021) 146505.
12. K.M. Huffman, T.R. Koves, M.J. Hubal, H. Abouassi, N. Beri, L.A. Bateman, R.D. Stevens, O.R. Ilkayeva, E.P. Hoffman and D.M. Muoio, *Diabetologia*, 57 (2014) 2282.
13. Z. Wang, T. Zhang, L. Pi, H. Xiang, P. Dong, C. Lu and T. Jin, *Colloids and Surfaces B: Biointerfaces*, 198 (2021) 111480.
14. R.A. Robergs, F. Ghiasvand and D. Parker, *American Journal of Physiology-Regulatory, Integrative and Comparative Physiology*, 278 (2004) R502.
15. P. Dong, T. Zhang, H. Xiang, X. Xu, Y. Lv, Y. Wang and C. Lu, *Journal of Materials Chemistry B*, 9 (2021) 958.
16. J. Rouhi, S. Mahmud, S.D. Hutagalung and N. Naderi, *Electronics letters*, 48 (2012) 712.
17. J. Sahuquillo, M.-A. Merino, A. Sánchez-Guerrero, F. Arikan, M. Vidal-Jorge, T. Martínez-Valverde, A. Rey, M. Riveiro and M.-A. Poca, *PLoS one*, 9 (2014) e102540.
18. T. Jiang, Z. Liu, G. Wang and Z. Chen, *Energy Reports*, 7 (2021) 3678.
19. N. Naderi, M. Hashim, J. Rouhi and H. Mahmodi, *Materials science in semiconductor processing*, 16 (2013) 542.
20. A. Bhide, K.-C. Lin, S. Muthukumar and S. Prasad, *Analyst*, 146 (2021) 3482.

21.   L. Zhang, J. Zheng, S. Tian, H. Zhang, X. Guan, S. Zhu, X. Zhang, Y. Bai, P. Xu and J. Zhang, *Journal of Environmental Sciences*, 91 (2020) 212.
22.   Q. Zhang, D. Jiang, C. Xu, Y. Ge, X. Liu, Q. Wei, L. Huang, X. Ren, C. Wang and Y. Wang, *Sensors and Actuators B: Chemical*, 320 (2020) 128325.
23.   A. Chen, K. Kamata, M. Nakagawa, T. Iyoda, H. Wang and X. Li, *The Journal of Physical Chemistry B*, 109 (2005) 18283.
24.   V.K.T. Ngo, D.G. Nguyen, T.P. Huynh and Q.V. Lam, *Advances in Natural Sciences: Nanoscience and Nanotechnology*, 7 (2016) 035016.
25.   S. Scorrano, L. Mergola, R. Del Sole and G. Vasapollo, *International journal of molecular sciences*, 12 (2011) 1735.
26.   R. Savari, H. Savaloni, S. Abbasi and F. Placido, *Sensors and Actuators B: Chemical*, 266 (2018) 620.
27.   M. Zhang, L. Zhang, S. Tian, X. Zhang, J. Guo, X. Guan and P. Xu, *Chemosphere*, 253 (2020) 126638.
28.   R.A. Anderson, M.M. Ariffin, P.A. Cormack and E.I. Miller, *Forensic science international*, 174 (2008) 40.
29.   F. Chahshouri, H. Savaloni, E. Khani and R. Savari, *Journal of Micromechanics and Microengineering*, 30 (2020) 075001
30.   C. Wang, F. Ye, H. Wu and Y. Qian, *International Journal of Electrochemical Science*, 8 (2013) 2440.
31.   P. Kuppusamy, S. Ilavenil, S. Srigopalram, D.H. Kim, N. Govindan, G.P. Maniam, M.M. Yusoff and K.C. Choi, *Journal of inorganic and Organometallic Polymers and Materials*, 27 (2017) 562.
32.   C. Shi, X. Zhang, X. Zhang, P. Chen and L. Xu, *Ultrasonics Sonochemistry*, 76 (2021) 105662.
33.   U. Jain, S. Soni, Y.P.S. Balhara, M. Khanuja and N. Chauhan, *ACS omega*, 5 (2020)
34.   S. Chen, L. Dong, M. Yan, Z. Dai, C. Sun and X. Li, *Royal Society open science*, 5 (2018) 171488.
35.   E.E. Elemike, D.C. Onwudiwe, O.E. Fayemi and T.L. Botha, *Applied Physics A*, 125 (2019) 1.
36.   Z. Zhang, J. Xu, Y. Wen, J. Zhang and W. Ding, *Synthetic Metals*, 230 (2017) 79.
37.   R. Savari, S. Soltanian, A. Noorbakhsh, A. Salimi, M. Najafi and P. Servati, *Sensors and Actuators B: Chemical*, 176 (2013) 335.
38.   B. Fresco-Cala, A.D. Batista and S. Cárdenas, *Molecules*, 25 (2020) 4740.
39.   H. Savaloni, R. Savari and S. Abbasi, *Current Applied Physics*, 18 (2018) 869.
40.   I. Bravo, M. Revenga-Parra, F. Pariente and E. Lorenzo, *Sensors (Basel, Switzerland)*, 17 (2017) 144.
41.   H. Cheng, T. Li, X. Li, J. Feng, T. Tang and D. Qin, *Journal of The Electrochemical Society*, 168 (2021) 087504.
42.   R.-C. Zhang, D. Sun, R. Zhang, W.-F. Lin, M. Macias-Montero, J. Patel, S. Askari, C. McDonald, D. Mariotti and P. Maguire, *Scientific reports*, 7 (2017) 1.
43.   H. Savaloni, E. Khani, R. Savari, F. Chahshouri and F. Placido, *Applied Physics A*, 127 (2021) 1.
44.   G. Vasapollo, R.D. Sole, L. Mergola, M.R. Lazzoi, A. Scardino, S. Scorrano and G. Mele, *International Journal of Molecular Sciences*, 12 (2011) 5908.
45.   A. Rico-Yuste and S. Carrasco, *Polymers*, 11 (2019) 1173.
46.   P. Manivel, V. Suryanarayanan, N. Nesakumar, D. Velayutham, K. Madasamy, M. Kathiresan, A.J. Kulandaisamy and J.B.B. Rayappan, *New Journal of Chemistry*, 42 (2018) 11839.
47.   T.C. Pereira and N.R. Stradiotto, *Microchimica Acta*, 186 (2019) 764.
48.   N. Nesakumar, S. Sethuraman, U.M. Krishnan and J.B.B. Rayappan, *Journal of Colloid and Interface Science*, 410 (2013) 158.
49.   M. Arivazhagan, A. Shankar and G. Maduraiveeran, *Microchimica Acta*, 187 (2020) 1.

50.   M. Gamero, M. Sosna, F. Pariente, E. Lorenzo, P.N. Bartlett and C. Alonso, *Talanta*, 94 (2012) 328.
51.   A.C. Pereira, M.R. Aguiar, A. Kisner, D.V. Macedo and L.T. Kubota, *Sensors and Actuators B: Chemical*, 124 (2007) 269.
52.   T. Shimomura, T. Sumiya, M. Ono, T. Ito and T.-a. Hanaoka, *Analytica chimica acta*, 714 (2012) 114.
53.   A. Stergiou, C. Stangel, R. Canton-Vitoria, R. Kitaura and N. Tagmatarchis, *Nanoscale*, 13 (2021) 8948.
54.   P.J. Derbyshire, H. Barr, F. Davis and S.P. Higson, *The journal of physiological sciences*, 62 (2012) 429.
55.   F. Pargar, H. Kolev, D.A. Koleva and K. van Breugel, *Advances in Materials Science and Engineering*, 2018 (2018) 1.